

DOE/PC/94208--T8

SEVENTH TECHNICAL PROGRESS REPORT

ON

HYDRODYNAMIC MODELS FOR SLURRY

BUBBLE COLUMN REACTORS

JANUARY - MARCH 1996

APRIL 1996

RECEIVED

OCT 28 1996

OSTI

U.S. DEPARTMENT OF ENERGY GRANT

DE-FG22-94PC4208

RECEIVED
USD OE/PETC
36 APR 30 PM 2:35
ACQUISITION & ASSISTANCE DIV.

DIMITRI GIDASPOW

PRINCIPAL INVESTIGATOR

DEPARTMENT OF CHEMICAL AND ENVIRONMENTAL ENGINEERING

ILLINOIS INSTITUTE OF TECHNOLOGY

CHICAGO, ILLINOIS 60616

MASTER

HH
DISTRIBUTION OF THIS DOCUMENT IS UNLIMITED

U.S. DOE PATENT CLEARANCE NOT REQUIRED

PRIOR TO PUBLICATION OF THIS REPORT

DISCLAIMER

This report was prepared as an account of work sponsored by an agency of the United States Government. Neither the United States Government nor any agency thereof, nor any of their employees, makes any warranty, express or implied, or assumes any legal liability or responsibility for the accuracy, completeness, or usefulness of any information, apparatus, product, or process disclosed, or represents that its use would not infringe privately owned rights. Reference herein to any specific commercial product, process, or service by trade name, trademark, manufacturer, or otherwise does not necessarily constitute or imply its endorsement, recommendation, or favoring by the United States Government or any agency thereof. The views and opinions of authors expressed herein do not necessarily state or reflect those of the United States Government or any agency thereof.

DISCLAIMER

**Portions of this document may be illegible
in electronic image products. Images are
produced from the best available original
document.**

HYDRODYNAMIC MODELS FOR SLURRY BUBBLE COLUMN REACTORS

ABSTRACT

The objective of this investigation is to convert our "learning gas-solid-liquid" fluidization model into a predictive design model. The IIT hydrodynamic model computes the phase velocities and the volume fractions of gas, liquid and particulate phase. Model verification involves a comparison of these computed velocities and volume fractions to experimental values.

This report presents the Ph.D. thesis of Mr. Y. Wu. All but a small fraction of his thesis dealt with the work of this project. A summary of his results are as follows.

A hydrodynamic model for multiphase flows, based on the principles of mass conservation, momentum balance and energy conservation for each phase, was developed and applied to model gas-liquid, gas-liquid-solid fluidization and gas-solid-solid separation. To simulate the industrial slurry bubble column reactors, a computer program based on the hydrodynamic model was written with modules for chemical reactions (e.g. the synthesis of methanol), phase changes and heat exchangers. Also the kinetic theory was programmed to compute the viscosity of the solid phase.


In the simulations of gas-liquid two phases flow system, the gas hold-ups, computed with a variety of operating conditions such as temperature, pressure, gas and liquid velocities, agree well with the measurements obtained at Air Products' pilot plant. The hydrodynamic model has more flexible features than the previous empirical correlations in predicting the gas hold-up of gas-liquid two-phase flow systems.

In the simulations of gas-liquid-solid bubble column reactors with and without slurry circulation, the code computes volume fractions, temperatures and velocity distributions for the gas, the liquid and the solid phases, as well as concentration distributions for the species (CO, H₂, CH₃OH, ...), after startup from a certain initial state. A kinetic theory approach is used to compute a solid viscosity due to particle collisions. Solid motion and gas-liquid-solid mixing are observed on a color PCSHOW movie made from computed time series data. The steady state and time average catalyst concentration profiles, the slurry height and the rates of methanol production agree well with the measurements obtained at an Air Products' pilot plant. The temperature movie shows heat transfer behavior of the internal heat exchangers. The simulations may be useful as a guide for industrial reactor design such as for determining reactor size, distributor design, positions of heat exchangers, mixing type, and erosion of heat exchanger tubes.

SIMULATION OF METHANOL SYNTHESIS
IN SLURRY BUBBLE COLUMN REACTORS

BY
YUANXIANG WU

Submitted in partial fulfillment of the
requirements for the degree of
Doctor of Philosophy in Chemical Engineering
in the Graduate College of the
Illinois Institute of Technology

Approved 
Adviser

Chicago, Illinois
May 1996

ACKNOWLEDGMENT

First, I would like to express my sincere appreciation and gratitude to my thesis advisor, Professor Dimitri Gidaspow, for his helpful advice and guidance during the course of this work.

Sincere thanks are due to my colleagues, Ms. Bing Sun, Professor Huilin Lu, Dr. Aubrey L. Miller, Dr. Isaac K. Gamwo, Dr. Apichai Therdthianwon, Dr. Mitra Bahary, Ms. Diana Matonis, Mr. Reza Mostafi and Mr. Augusto Neri, for their help and cooperation.

Furthermore, my thanks are extended to the staff of the Department of Chemical and Environmental Engineering in IIT for their support.

Finally and most specially, I would like to thank my wife Hongli for her invaluable support and encouragement during the pursuit of my doctorate.

Financial support for this study was provided by the US Department of Energy Grant No. DE-FG22-94PC94208.

Y. W.

TABLE OF CONTENTS

	Page
ACKNOWLEDGMENT	iii
LIST OF TABLES	vi
LIST OF FIGURES	vii
LIST OF SYMBOLS	xii
ABSTRACT	xv
 CHAPTER	
I. INTRODUCTION	1.1
II. DESCRIPTIONS OF HYDRODYNAMIC MODELS	2.1
2.1 Introduction	2.1
2.2 Hydrodynamic Models	2.1
2.3 Constitutive Equations	2.3
2.4 Solid Viscosity from Kinetic Theory Approach	2.6
2.5 Reaction and Mass Transfer	2.8
2.6 Species Balances	2.8
III. GAS HOLDUP OF GAS-LIQUID FLUIDIZATION	3.1
3.1 Introduction	3.1
3.2 Hydrodynamic Models	3.2
3.3 Operating Conditions	3.4
3.4 Numerical Considerations	3.5
3.5 Results and Discussions	3.8
IV. METHANOL SYNTHESIS WITH SLURRY CIRCULATION	4.1
4.1 Introduction	4.1
4.2 Reaction Kinetics and Mass Transfer	4.1
4.3 Species Balance.	4.3
4.4 Mathematical Models (Empirical)	4.3
4.5 Operation Conditions	4.5
4.6 Numerical Considerations	4.6
4.7 Computational Results and Discussions	4.9

CHAPTER	Page
V. METHANOL SYNTHESIS WITHOUT SLURRY CIRCULATION	5.1
5.1 Introduction	5.1
5.2 Reaction and Kinetic Model	5.1
5.3 Mathematics Models (Kinetic Theory)	5.2
5.4 Operation Conditions	5.6
5.5 Numerical Considerations	5.8
5.6 Computational Results and Discussions	5.11
5.7 Convergence Check	5.20
VI. SEPARATION OF PYRITE FROM COAL IN AN INCLINED ELECTRO-FLUIDIZED BED	6.1
6.1 Introduction	6.1
6.2 Hydrodynamic Model	6.4
6.3 Operation Conditions	6.7
6.4 Numerical Considerations	6.7
6.5 Computational Results and Discussions	6.12
VII. SUMMARY AND RECOMMENDATIONS	7.1
APPENDIX	
A. NUMERICAL BASIS OF PROGRAM MFREK	A.1
B. ORGANIZATION AND USER MENU OF MFREK	B.1
C. SOURCE FORTRAN CODE OF MFREK AND A SAMPLE INPUT DATA	C.1
BIBLIOGRAPHY	D.1

LIST OF TABLES

Table	Page
3.1 Computed and Measured Gas Holdups at Reactor Height 137cm	3.6
4.1 Material Balance: (CO:H ₂ =1:3)	4.9
4.2 Comparison of Simulation and Air Products' (1987) RUN E-2-B	4.10
5.1 Material Balance: (CO:H ₂ =1.5:1)	5.12
5.2 Comparison of Simulation and Air Products' (1991) RUN E-8.1	5.12
6.1 Case 1: Dense Operation with High Pyrite Content	6.9
6.2 Case 2: Dense Operation with Low Pyrite Content	6.9
6.3 Case 3: Pneumatic Operation	6.9

LIST OF FIGURES

Figure	Page
3.1 Reactor Operation and Simulation Grid	3.7
3.2 Computed and Experimental Gas Holdup Profiles	3.9
3.3 Computed and Experimental Axial Gas Holdup Profiles (Effect of Liquid Velocity)	3.11
3.4 Computed and Experimental Gas Holdup vs Gas Velocity (at Reactor Height=137cm)	3.12
3.5 Effect of Temperature on Gas Holdup (at Reactor Height=137cm)	3.13
3.6 Effect of Pressure on Gas Holdup (at Reactor Height=137cm)	3.14
3.7 Comparison of Experimental and Computed Gas Holdup	3.15
4.1 Reactor Operation with Slurry Circulation and Simulation Grid	4.8
4.2 Computed and Experimental Axial Catalyst Volume Fraction Profiles	4.11
4.3 Computed Gas, Liquid and Solid Axial Volume Fraction Profiles	4.12
4.4 Computed Axial Methanol Concentration Profile	4.13
4.5a The Catalyst Concentration Profiles as a Function of Time	4.14
4.5b The Catalyst Concentration Profiles as a Function of Time	4.15
4.5c The Catalyst Concentration Profiles as a Function of Time	4.16
4.6a The Methanol Concentration Profiles as a Function of Time	4.17
4.6b The Methanol Concentration Profiles as a Function of Time	4.18
4.6c The Methanol Concentration Profiles as a Function of Time	4.19
5.1 Reactor Operation without Slurry Circulation and Simulation Grid	5.7
5.2 Gas Mass Flowrate at Reactor Top	5.13

Figure	Page
5.3 Time average G-L-S Volume Fraction Profiles	5.14
5.4 Methanol Concentration Profiles from IIT's Hydrodynamic, One-dimensional and Vikings' Models	5.15
5.5a The Gas Volume Fraction Profiles as a Function of Time	5.16
5.5b The Gas Volume Fraction Profiles as a Function of Time	5.17
5.5c The Gas Volume Fraction Profiles as a Function of Time	5.18
5.5d The Gas Volume Fraction Profiles as a Function of Time	5.19
5.6a The Solid Volume Fraction Profiles as a Function of Time	5.21
5.6b The Solid Volume Fraction Profiles as a Function of Time	5.22
5.6c The Solid Volume Fraction Profiles as a Function of Time	5.23
5.6d The Solid Volume Fraction Profiles as a Function of Time	5.24
5.7a The Methanol Concentration Profiles as a Function of Time	5.25
5.7b The Methanol Concentration Profiles as a Function of Time	5.26
5.7c The Methanol Concentration Profiles as a Function of Time	5.27
5.7d The Methanol Concentration Profiles as a Function of Time	5.28
5.7e The Methanol Concentration Profiles as a Function of Time	5.29
5.8a The Temperature Profiles as a Function of Time	5.30
5.8b The Temperature Profiles as a Function of Time	5.31
5.8c The Temperature Profiles as a Function of Time	5.32
5.9 Instant Rate of Reaction (gmol/s/cm^3)	5.33
5.10 Solid Viscosity Distribution	5.34
5.11 Solid Granular Temperature	5.35
5.12 Gas Transient Flow Pattern	5.36

Figure	Page
5.13 Time Series of Gas Flow Patterns	5.37
5.14 Time Average G-L-S Volume Fraction Profiles in Different Grid	5.39
5.15 Gas Flowrate at Reactor Top and Frequence Response (Fine Grid)	5.40
5.16 Gas Flowrate at Reactor Top and Frequence Response (Coarse Grid)	5.41
5.17a Gas Flow Patterns (Fine Grid)	5.42
5.17b Gas Flow Patterns (Fine Grid)	5.43
5.18a Gas Flow Patterns (Coarse Grid)	5.44
5.18b Gas Flow Patterns (Coarse Grid)	5.45
6.1 Simulation Grid of an Inclined Electro-Fluidized Bed	6.8
6.2 Coal Recovery vs Pyrite Content of Coal	6.13
6.3a Pyrite and Coal Volume Fraction Profiles and Flow 48 Patterns. Dense Case: Air/Coal (21.6% Pyrite) = 1/1	6.14
6.3b Pyrite and Coal Volume Fraction Profiles and Flow Patterns. Dense Case: Air/Coal (2.5% Pyrite) = 1/1	6.15
6.3c Pyrite and Coal Volume Fraction Profiles and Flow Patterns. Dilute Case: Air/Coal (1.7% Pyrite) = 1/0.012	6.16
6.4a The Coal Volume Fraction Profiles as a Function of Time (Case 2)	6.18
6.4b The Coal Volume Fraction Profiles as a Function of Time (Case 2)	6.19
6.4c The Coal Volume Fraction Profiles as a Function of Time (Case 2)	6.20
6.4d The Coal Volume Fraction Profiles as a Function of Time (Case 2)	6.21
6.4e The Coal Volume Fraction Profiles as a Function of Time (Case 2)	6.22
6.4f The Coal Volume Fraction Profiles as a Function of Time (Case 2)	6.23
6.5a The Pyrite Volume Fraction Profiles as a Function of Time (Case 2)	6.24
6.5b The Pyrite Volume Fraction Profiles as a Function of Time (Case 2)	6.25

Figure	Page
6.5c The Pyrite Volume Fraction Profiles as a Function of Time (Case 2) . . .	6.26
6.5d The Pyrite Volume Fraction Profiles as a Function of Time (Case 2) . . .	6.27
6.5e The Pyrite Volume Fraction Profiles as a Function of Time (Case 2) . . .	6.28
6.5f The Pyrite Volume Fraction Profiles as a Function of Time (Case 2) . . .	6.29
6.6a The Coal Flow Patterns as a Function of Time (Case 2)	6.30
6.6b The Coal Flow Patterns as a Function of Time (Case 2)	6.31
6.6c The Coal Flow Patterns as a Function of Time (Case 2)	6.32
6.6d The Coal Flow Patterns as a Function of Time (Case 2)	6.33
6.6e The Coal Flow Patterns as a Function of Time (Case 2)	6.34
6.6f The Coal Flow Patterns as a Function of Time (Case 2)	6.35
6.7a The Pyrite Flow Patterns as a Function of Time (Case 2)	6.36
6.7b The Pyrite Flow Patterns as a Function of Time (Case 2)	6.37
6.7c The Pyrite Flow Patterns as a Function of Time (Case 2)	6.38
6.7d The Pyrite Flow Patterns as a Function of Time (Case 2)	6.39
6.7e The Pyrite Flow Patterns as a Function of Time (Case 2)	6.40
6.7f The Pyrite Flow Patterns as a Function of Time (Case 2)	6.41
6.8a The Coal Flow Patterns as a Function of Time (Case 1)	6.42
6.8b The Coal Flow Patterns as a Function of Time (Case 1)	6.43
6.8c The Coal Flow Patterns as a Function of Time (Case 1)	6.44
6.8d The Coal Flow Patterns as a Function of Time (Case 1)	6.45
6.9a The Pyrite Flow Patterns as a Function of Time (Case 1)	6.46
6.9b The Pyrite Flow Patterns as a Function of Time (Case 1)	6.47

Figure	Page
6.9c The Pyrite Flow Patterns as a Function of Time (Case 1)	6.48
6.9d The Pyrite Flow Patterns as a Function of Time (Case 1)	6.49
6.10a The Coal Flow Patterns as a Function of Time (Case 3)	6.50
6.10b The Coal Flow Patterns as a Function of Time (Case 3)	6.51
6.10c The Coal Flow Patterns as a Function of Time (Case 3)	6.52
6.10d The Coal Flow Patterns as a Function of Time (Case 3)	6.53
6.10e The Coal Flow Patterns as a Function of Time (Case 3)	6.54
6.11a The Pyrite Flow Patterns as a Function of Time (Case 3)	6.55
6.11b The Pyrite Flow Patterns as a Function of Time (Case 3)	6.56
6.11c The Pyrite Flow Patterns as a Function of Time (Case 3)	6.57
6.11d The Pyrite Flow Patterns as a Function of Time (Case 3)	6.58
6.11e The Pyrite Flow Patterns as a Function of Time (Case 3)	6.59
6.12 The Coal Viscosity vs Concentration (Dense Case)	6.61
6.13 The Pyrite Viscosity vs Concentration (Dense Case)	6.62
6.14 The Pyrite Viscosity vs Concentration (Dilute Case)	6.63
6.15 Comparison of Coal and Pyrite viscosities (Dense Case)	6.64
A.1 The Computational Mesh	A.9
A.2 The Staggered Computational Mesh for Momentum equations	A.11
A.3 The Computational Sweep	A.19
A.4 The Secant method for Pressure Iteration	A.22
B.1 The Program Flow Chart	B.3

LIST OF SYMBOLS

Symbol	Definition
A	coefficient matrix
a	interfacial area per unit volume (cm^2/cm^3)
B	coefficient matrix
C_D	drag coefficient
C_j^l	concentration of j in bulk liquid phase
C_j^{g-l}	concentration of j in g-l interface
C_k	fluctuating velocity of particle
C_{pg}	specific heat of gas
C_{pk}	specific heat of phase k
d_k	diameter of solid particle or liquid droplet
e_k	restitution coefficient of phase k
F_g	forces acting on gas phase
F_k	forces acting on phase k
E	strength of electric field
f_j	fugacity of j
H_j	Henry's constant of j
H_g	enthalpy of gas
H_k	enthalpy of phase k
h_{vk}	gas-phase k heat transfer coefficient
$G(\)$	solid compressive stress modules
g	gravity acceleration
\mathcal{G}_{0k}	radial distribution of phase k
[I]	unit tensor
K_{eq}	reaction equilibrium constant
K_r	reaction kinetic coefficient
K_{j^l}	mass transfer coefficient of j in liquid phase
k_g	thermal conductivity of gas

Symbol	Definition
k_k	thermal conductivity of phase k
k_g^0	mean thermal conductivity of gas
k_k^0	mean thermal conductivity of phase k
k_k^*	effective thermal conductivity of phase k
M^j	molecular weight of j
\bar{M}_g	average gas molecular weight
M_k	number of reactions in phase k
\dot{m}_k	rate of generation of phase k
N	total number species
Nu_k	Nusselt number
P_g	gas pressure
P_k	pressure of phase k
Pr	Prandtl number
q_k	surface charge of phase k
r_{ik}	rate of ith reaction in phase k
R	gas constant
R_k^j	rate of mass transfer, j specie in phase k
Re_k	Reynolds number
T	temperature
T_g	gas temperature
T_k	temperature of phase k
T_g^0	reference gas temperature
T_k^0	reference temperature of phase k
u	velocity in x direction
v	velocity in y direction
y_k^j	weight fraction of i in phase k
z	compressible factor

Greek letters:

α_{ik}^j stoichiometric coefficient of ith reaction in k phase ξ_k

Symbol	Definition
β_{kl}	frictional coefficient between phase k and l
γ_k	collisional energy dissipation
ΔH_{ik}	reaction heat of ith reaction in phase k
ε_k	volume fraction of phase k
Θ	granular temperature
κ_k	conductivity of fluctuating energy
μ_k	viscosity of phase k
ξ_k	bulk viscosity
ρ_k	density of phase k
τ_{ck}	cohesive force
τ_k	shear stress of phase k
Φ_k	energy dissipation
Ψ_k	sphericity of particle or droplet

Subscripts:

g, l, s	gas, liquid, solid respectively
i	ith reaction
k	solid or liquid phase

Superscripts

j	species
-----	---------

ABSTRACT

In this study, a hydrodynamic model for multiphase flows, based on the principles of mass conservation, momentum balance and energy conservation for each phase, was developed and applied to model gas-liquid, gas-liquid-solid fluidization and gas-solid-solid separation. To simulate the industrial slurry bubble column reactors, a computer program based on the hydrodynamic model was written with modules for chemical reactions (e.g. the synthesis of methanol), phase changes and heat exchangers. Also the kinetic theory was programmed to compute the viscosity of the solid phase.

The slurry bubble column reactor, a typical multiphase flow system, is used to produce methanol from syn-gas (CO, H₂, ...). The hydrodynamic model was used to simulate the reactor's time-dependent dynamic behavior. The code computes volume fractions, temperatures and velocity distributions for the gas, the liquid and the solid phases, as well as concentration distributions for the species (CO, H₂, CH₃OH, ...), after startup from a certain initial state. In this simulation, the gas is treated as a continuous phase while the solid (catalyst) and the liquid (wax) as a dispersed phase. A kinetic theory approach is used to compute a solid viscosity due to particle collisions. Solid motion and gas-liquid-solid mixing are observed on a color PCSHOW movie made from computed time series data. The steady state and time average catalyst concentration profiles and the rate of methanol production agree well with the measurements obtained at an Air Products' pilot plant. The temperature movie shows heat transfer behavior of the internal heat exchangers. The simulations may be useful as a guide for industrial reactor design

such as for determining reactor size, distributor design, positions of heat exchangers, mixing type, and erosion of heat exchanger tubes.

The model was also applied to understand the hydrodynamics of electrostatic separation of pyrites from coal. The model was modified to include an external electric force. The kinetic theory has been applied to predict the viscosities for both solid phases, coal and pyrites. The study showed that pyrites can be removed from coal in an inclined electro-fluidized bed. A series of pictures from simulations show the hydrodynamic behavior, such as solid flow patterns and pyrites concentrations, in the electrostatic separator. This study indicates that dilute feeding results a high coal recovery and leads to an improved design of electrostatic separators.